

Targeting CCR3 to Reduce Amyloid- β Production, Tau Hyperphosphorylation, and Synaptic Loss in a Mouse Model of Alzheimer's Disease

Chunyan Zhu¹ · Bing Xu² · Xiaohong Sun³ · Qiwen Zhu⁴ · Yi Sui^{2,3,4}

Received: 16 July 2016 / Accepted: 30 October 2016 / Published online: 23 November 2016
© Springer Science+Business Media New York 2016

Abstract The majority of Alzheimer's disease (AD) patients have a late onset, and chronic neuroinflammation, characterized by glial activation and secretion of pro-inflammatory cytokines and chemokines, plays a role in the pathogenesis of AD. The chemokine CCL11 has been shown to be a causative factor of cognitive decline in the process of aging, but little is known whether it is involved in the pathogenesis of AD. In the present study, we showed that CCR3, the receptor for CCL11, was expressed by hippocampal neurons and treatment of primary hippocampal neuronal cultures (14 days *in vitro*) with CCL11 resulted in activation of cyclin-dependent kinase 5 and glycogen synthase kinase-3 β , associated with elevated tau phosphorylation at multiple sites. CCL11 treatment also induced the

production of A β and dendritic spine loss in the hippocampal neuronal cultures. All these effects were blocked by the CCR3 specific antagonist, GW766994. An age-dependent increase in CCL11, predominantly expressed by the activated microglia, was observed in the cerebrospinal fluid of both APP/PS1 double transgenic mice and wild-type (WT) littermates, with a markedly higher level in APP/PS1 double transgenic mice than that in WT littermates. Deletion of CCR3 in APP/PS1 double transgenic mice significantly reduced the phosphorylation of CDK5 and GSK3 β , tau hyperphosphorylation, A β deposition, microgliosis, astrogliosis, synaptic loss, and spatial learning and memory deficits. Thus, the age-related increase in CCL11 may be a risk factor of AD, and antagonizing CCR3 may bring therapeutic benefits to AD.

✉ Yi Sui
jakeyisui@icloud.com

Chunyan Zhu
syzy1965@sina.com

Bing Xu
wlt1967@sina.com

Xiaohong Sun
cmu4h_sxh@126.com

Qiwen Zhu
qwzhu18@163.com

Keywords CCR3 · Alzheimer's disease · CCL11 · β -amyloid · Tau · Hyperphosphorylation · Synapse

Introduction

Alzheimer's disease (AD), the leading cause of dementia in the elderly, is a progressive brain disorder affecting regions of the brain that control cognitive functions. The major pathologic hallmarks of AD include senile plaques, which are formed by extracellular deposition of amyloid β (A β) surrounded by astrocytes and microglia; intracellular accumulation of neurofibrillary tangles, which are composed of the hyperphosphorylated tau; and the loss of neurons and synapses [22, 30]. The vast majority of AD cases have a late onset, and delaying the age at onset with therapeutic or prophylactic approaches would have significant benefits [4]. However, as mechanisms underlying the pathology of AD remain largely unclear, no therapies have been successful in achieving this important goal.

¹ Department of Neurology, Shenyang Seventh People's Hospital, Shenyang, China

² Department of Neurology, Shenyang First People's Hospital, Shenyang Brain Hospital, Shenyang Brain Institute, Shenyang, China

³ Department of Neurology, the Fourth Affiliated Hospital, China Medical University, Shenyang, China

⁴ Key laboratory of Behavioral and Cognitive Neuroscience of Liaoning Province, Shenyang Medical College, Shenyang, China

Increasing lines of evidence indicate that neuroinflammation, promoted by the activated astrocytes and microglia, which produce pro-inflammatory cytokines, chemokines, and neurotoxins, appears to play an important role in the pathogenesis of AD [18]. Because of their critical roles in the regulation of neuron-microglia crosstalk, chemokines have attracted increasing attention in AD studies [25]. Different chemokines may play diverse roles in the pathogenesis of AD. For instance, whereas CXCR2 is involved in A β production and tau pathology [3, 47], CX3CR1 appears to protect against AD-related cognitive dysfunction linked to aberrant microglial activation and excessive production of pro-inflammatory cytokines [6]. Thus, understanding the complex roles of chemokines in AD pathology may provide significant insight into the mechanisms of AD and may lead to development of novel therapeutic approaches for AD.

Besides the extensively studied chemokines described above, CCL11 is another chemokine potentially involved in AD pathology. CCL11 has been shown to be gradually elevated in the serum during the process of aging, and its age-dependent increase is correlated with deficits in hippocampus-dependent learning and memory tasks [39]. The effects of aging on these parameters could be replicated by intracerebroventricular injection of recombinant CCL11 and could be prevented by systemic or intracerebroventricular administration of neutralizing antibodies for CCL11 [39]. Thus, CCL11 is likely a key player in hippocampal function—with great relevance to AD. CCL11 binds to CCR3, a chemokine receptor known to be expressed by astrocytes, microglia, and neurons [16, 17, 38, 46]. Though CCR3 has been shown to play a role in microglial activation [10], given its neuronal expression, it is reasonably hypothesized that CCL11/CCR3 might be involved in the neuronal dysfunctions during AD pathogenesis.

In the present study, we demonstrate that CCL11 treatment resulted in marked activation of cyclin-dependent kinase 5 (CDK5) and glycogen synthase kinase-3 β (GSK-3 β), both of which are key regulators in the hyperphosphorylation of tau, leading to neurofibrillary tangle formation, and also important players in the phosphorylation and the subsequent cleavage of amyloid precursor protein (APP), leading to the generation of A β [7]. As a result, CCL11 enhanced tau phosphorylation and the production of amyloid β (A β), associated with dendritic spine loss in hippocampal neuronal cultures. APP and presenilin 1 (PS1) double-transgenic (APP/PS1) mice deficient in CCR3 exhibited significantly reduced A β deposition and the associated gliosis, tau hyperphosphorylation, and synaptic loss, associated with improvement in learning and memory. Thus, the age-related increase in CCL11/CCR3 may be involved in AD pathogenesis, and antagonizing CCR3-mediated tau hyperphosphorylation, A β production, and synaptic loss may bring therapeutic benefits to AD.

Materials and Methods

Animals CCR3^{-/-} and APP/PS1 double-transgenic mice (B6C3-Tg [APP^{swe},PSEN1^{dE9}] 85Dbo/J) expressing a chimeric mouse/human APP (Mo/HuAPP695^{swe}) and a mutant human PS1 (PS1-dE9) protein mice were purchased from The Jackson Laboratory (Bar Harbor, ME, USA). These mice were backcrossed at least eight generations to the C57BL/6 strain. To obtain CCR3-deficient mice with a transgenic expression of APP/PS1 (APP/PS1/CCR3^{-/-}), heterozygous APP/PS1 mice were successively crossed with CCR3^{-/-} mice and subsequently intercrossed. Only male mice were studied in order to avoid possible influence of sex on amyloid plaque formation and inflammation in AD. All animals were housed according to standard animal care protocols and maintained in a pathogen-free environment at the Shenyang First People's Hospital. The animals were randomized for therapy trials and coded, and the operators and data analyzer remained double blinded to which treatment they received, until the code was broken at the completion of data collection. All procedures were performed in accordance with the Shenyang First People's Hospital Institutional Animal Care and Use Committee and followed the National Institutes of Health guide for the care and use of Laboratory animals (NIH Publications No. 8023, revised 1978).

Morris Water-Maze Test Twelve-month-old WT, CCR3^{-/-}, APP/PS1, and APP/PS1/CCR3^{-/-} mice were tested using the Morris water maze [33]. Briefly, mice were placed into the water in a quasi-random fashion and were allowed to search for the platform for 120 s. Once reaching the platform, the mice were allowed to remain on it for 10 s. If a mouse failed to locate the platform within 120 s, it was assisted by the experimenter to stand on the platform for the same period of time. After the trial, the mice were taken out, dried, and placed in a separate cage for ~60 min until the next trial. Mice were trained for four trials per day for five consecutive days, and their spatial learning scores (latency in seconds to find the platform) were recorded. In spatial probe trials conducted 24 h after the last training session (day 5), the platform was removed and the mice were allowed to swim freely for 90 s, and time spent in the target quadrant was recorded. All movements were recorded by a computerized tracking system (Noldus, Ethovision 3.1).

Immunohistochemistry Immunohistochemistry was performed as described previously [9]. Briefly, animals were killed with an overdose of xylazine (3 mg/kg) and ketamine (30 mg/kg) and their brains removed. The brains were fixed in phosphate-buffered saline (PBS) containing 4% paraformaldehyde and 15% glycerol cryoprotectant. Sections (50 μ m) were cut on a freezing microtome. Sections were washed extensively in PBS and processed as free-floating slices.

Permeabilization and blocking were achieved by incubation of the sections for 1 h at room temperature in PBS containing 0.5% Triton X-100 (vol/vol) and 3% bovine serum albumin. After rinsing, the primary antibody was developed by incubating with cyanine 3 (Cy3)- or Alexa 488-conjugated secondary antibodies against the corresponding species or by incubating with biotinylated secondary antibodies against the corresponding species for 1 h at room temperature, followed by DAB (Vector Laboratories) staining according to the manufacturer's instruction. The following antibodies were used: mouse monoclonal anti-CCR3 (ab36827, Abcam), mouse monoclonal anti-p-tau (T181) antibody (ab38505, Abcam), mouse monoclonal anti-A β 42 (6E10; Signet), rabbit polyclonal glial fibrillary acidic protein (GFAP) antibody (Dako Cytomation), rabbit polyclonal Iba-1 antibody (Wako Pure Chemicals), rabbit polyclonal microtubule associated protein 2 (MAP2) antibody (Millipore Bioscience Research Reagents). Primary antibodies were applied at dilutions of 1:3000 for GFAP, 1:1000 for MAP2, 1:500 for A β 42, 1:200 for Iba-1, 1:100 for CCR3, and 1:300 for p-tau (T181).

Stereological Analysis The stereological analysis was performed under a fluorescence or light microscope with oil immersion $\times 100$ objectives. The number of A β plaques, astrocytes, microglia, and p-Tau-positive neurons in the hippocampal region were counted using the optical fractionator method of unbiased stereological cell counting techniques as described previously [8, 9, 44].

Western Blot Analysis Samples were prepared as described previously [8, 9]. Briefly, cells or brain tissues were homogenized in Tris-buffered saline (TBS) (20 mM Tris-HCl buffer, pH 7.4, 150 mM NaCl) containing a mixture of protease inhibitors, including 0.5 mM phenylmethylsulfonyl fluoride, 20 μ g/ml aprotinin, 20 μ g/ml leupeptin, 20 μ g/ml pepstatin, and 1 mM EDTA (all inhibitors obtained from Sigma). Homogenates were sonicated briefly and centrifuged at 15,000 $\times g$ for 30 min. Samples (10 μ g of protein per lane) were run on 10% SDS polyacrylamide gel under reducing conditions. Proteins were transferred to a polyvinylidene difluoride (GE Healthcare) membrane. The membrane was blocked with TBS containing 0.1% Tween 20, 3% dry milk for 1 h before being incubated at room temperature for 2 h with specific antibodies. After washing, blots were incubated with the corresponding HRP-labeled secondary antibodies (1:1000 dilution) for 1 h. Labeling was detected using the ECL system (GE Healthcare). Bands were analyzed using densitometric software (Scion Image). The following antibodies were used for Western blot: rabbit polyclonal anti-APP-terminal fragments (CTFs) (Sigma), mouse monoclonal anti-p-tau (T181) (1:500; Abcam), rabbit polyclonal anti-p-tau (T205) (1:1000; Santa Cruz Biotechnology), rabbit polyclonal anti-p-tau (Ser199) (1:1000; Santa Cruz Biotechnology), rabbit polyclonal anti-p-tau (Ser235) (1:1000; Santa Cruz

Biotechnology), mouse monoclonal anti-cyclin-dependent kinase 5 (CDK5) (1:1000; Santa Cruz Biotechnology), mouse monoclonal anti-p-ERK1/2 (1:1000; Santa Cruz Biotechnology), mouse monoclonal anti-p-CDK5 (Ser159) (1:200; Santa Cruz Biotechnology), mouse monoclonal anti-p-glycogen synthase kinase 3 β (GSK3 β) (Ser9) (1:1000; Santa Cruz Biotechnology), mouse monoclonal anti-phospho-GSK3 α/β (Tyr279/216) (1:1000; ECM Biosciences), rabbit polyclonal anti-tau (1:1000; Santa Cruz Biotechnology), mouse monoclonal anti-GSK3 β (1:4000; Sigma), mouse monoclonal anti-ERK2 (1:1000; Santa Cruz Biotechnology), mouse monoclonal anti- β -actin (1:4000; Sigma), mouse monoclonal anti-Drebrin (1:15,000; DakoCytomation), and mouse monoclonal anti-PSD95 (1:1000; DakoCytomation).

Golgi-Cox Staining and the Number of Dendritic Spine Assay

The experiments were performed as described previously [11]. Briefly, the brains were stored in dark room in Golgi-Cox staining solution at 37 °C for 48 h, and brain slices were cut at the thickness of 200 μ m with a vibratome (VT1000S, Leica, Germany). The slices were stained with the following steps: (1) ammonia for 60 min, (2) water for three times, and (3) Kodak Film Fix for 30 min. After the staining, the slices were washed, dehydrated, and mounted using a resinous medium. The hippocampal neurons were imaged using a $\times 10$ or $\times 100$ objective with a Nikon wide field microscope (Eclipse 80i). Dendritic length and the number of mushroom spines within those neurons were analyzed by Matlab software.

Electron Microscopy Sample preparation and electron microscopy were performed as described previously [14]. Briefly, animals were sacrificed with an overdose of ketamine (30 mg/kg) and xylazine (3 mg/kg), and perfused with 2.5% glutaraldehyde/2% paraformaldehyde in 0.1 M sodium cacodylate buffer (pH 7.4). The hippocampus was sliced into 1-mm slices and post-fixed with 1.5% potassium ferrocyanide and 1% osmium tetroxide for 1 h. After washing, the slices were incubated in 1% aqueous uranyl acetate for 1 h, before being dehydrated in gradient alcohol (50, 70, 90, and 100%, 10 min each). The samples were placed in propylene oxide for 1 h, followed by infiltration overnight in TAAB Epon and propylene oxide (1:1 mixture). The samples were then embedded in TAAB Epon and polymerized at 60 °C for 48 h. Ultrathin sections were cut on a Reichert Ultracut-S microtome before being stained with uranyl acetate and lead citrate. Images were recorded with an AMT 2 k CCD camera. For each animal, 20 distinct apical regions of CA1, approximately 50–100 μ m from the cell body layer of the hippocampus was imaged. A synapse was defined as an electron-dense post-synaptic density area juxtaposed to a pre-synaptic terminal filled with synaptic vesicles.

Primary Neuronal Culture and Transfection Primary hippocampal neuronal cultures were prepared from rat fetuses at embryonic days 18–19 according to previously established protocols [13]. The embryonic rat hippocampal tissues were dissected under surgical microscope and digested with 0.15% trypsin for 10–15 min at 37 °C. The digestion was ended by adding DMEM supplemented with 10% fetal bovine serum. The hippocampal neuronal suspensions were filtered with 70- μ m cell strainers, before being plated in culture plates with or without poly-D-lysine hydrobromide-coated coverslips. Cells were maintained in DMEM supplemented with 10% FBS and 1% Pen/Strep. Twelve hours after plating, the medium was replaced with Neurobasal media containing 2% B27 supplement, 1% Glutamax, and 1% Pen/Strep. For morphological studies, the neuronal cultures were transiently transfected with EGFP vector at 7 DIV by using Lipofectamine 2000. Neurons (14 days in vitro) grown on coverslips were washed with PBS and fixed in 4% formaldehyde (pH 7.4) for 15 min at room temperature, before being mounted on glass slides with SlowFade Light reagent (Molecular Probes, Eugene, OR).

ELISA Analysis of A β Levels in Primary Hippocampal Neuronal Cultures A highly sensitive sandwich ELISA kit (Immuno-Biological Laboratories, Gunma, Japan) was used to measure the concentration of A β in the medium of primary cell cultures. Briefly, monoclonal rabbit anti-human IgGs anti-A β _{35–40} or anti-A β _{38–42} were used to capture A β _{1–40} and A β _{1–42}, respectively, from an equal amount of each CM sample. The horseradish peroxidase-conjugated anti-human A β _{11–28} Fab was used for detection in both assays [24]. This detection antibody recognizes both integral and N-terminus-cleaved variants of A β _{1–40} and A β _{1–42}. The measurement range for A β _{1–40} and A β _{1–42} was 4–231 pM and 3–178 pM, respectively.

Immunocytochemistry and Confocal Microscopy Immunocytochemistry was performed as described previously [47]. Briefly, cells were fixed with PBS (pH 7.4) containing 4% paraformaldehyde for 15 min and were then membrane-permeabilized with 0.5% Triton X-100 in PBS for 5 min. After being blocked with 3% bovine serum albumin at 37 °C for 1 h, the cells were incubated with the following primary antibodies: rabbit polyclonal anti-MAP2 antibody (1:200, Sigma) and mouse monoclonal anti-CCR3 antibody (1:200, Santa Cruz), at 4 °C overnight. Cells were then incubated with secondary antibodies conjugated to either cyanine 3 (Cy3, 1:500; Jackson ImmunoResearch) or Alexa 488 (1:500; Molecular Probes). Fluorescent images were obtained using an LSM 510 Zeiss microscope with a \times 25 or a \times 63 water-immersion objective lens. All images were taken at 512 \times 512 pixel resolution.

Collection of CSF and Measurement of CCL11 in CSF Mice were anesthetized with ketamine/xylazine mixture (100 mg/kg ketamine, 10 mg/kg xylazine, i.p.) and positioned in a stereotaxic frame (RWD Life Science, Shenzhen, China). A cervical incision was made with a microcapillary, which penetrated the atlanto-occipital membrane of the cisterna magna until CSF was obtained. Approximately 5–8- μ l CSF was collected from each mouse. To avoid blood contamination, the abundance of hemoglobin, catalase, peroxiredoxin, and carbonic anhydrase I, the blood-specific highly abundant proteins, were measured in each CSF sample as a standard procedure and CSF samples contaminated with blood were excluded.

To measure CXCL1 levels in CSF, CSF was diluted in the sample buffer provided by the manufacturer. For Luminex assay, 50 μ l of diluted CSF was loaded to each well of the 96-well assay plate containing the capturing antibody-bound beads. One hour after the incubation, the plates were washed and the diluted biotinylated detection antibody was added. After incubation for 30 min, the plates were washed and incubated with diluted streptavidin-R-PE for 10 min. Levels of CXCL1 were quantified with a Luminex 200 Workstation (Bio-rad, Hercules, CA).

Statistical Analysis Data are expressed as the mean \pm SEM. Analyses were performed using a two-way ANOVA followed by Fisher's least significant difference post hoc analysis to identify significant effects. Differences were considered significant at $p < 0.05$.

Results

CCL11 Induces CDK5 and GSK3 β Activation, Tau Phosphorylation, A β Production, and Dendritic Spine Loss in Hippocampal Neuronal Cultures To determine whether CCL11 causes neuronal dysfunctions associated with AD, we first examined whether its receptor CCR3 is expressed by 14 DIV hippocampal neurons. The rationale for using 14 DIV neurons is that neurons are relatively mature at this stage based on our observations. Co-immunostaining of hippocampal neuronal cultures (14 DIV) with anti-CCR3 and anti-MAP2 antibodies demonstrated a co-localization between CCR3- and MAP-expressing neurons (Fig. 1a), whereas immunostaining with an isotype control IgG did not show the CCR3 signal (Fig. 1a), suggesting specific expression of CCR3 in the neurons. By counting 200 neurons in each group, we observed 100% neurons expressed CCR3. CCL11 treatment resulted in the activation of CDK5, a protein kinase that plays important roles in AD pathogenesis [19], in the hippocampal neurons from WT but not CCR3^{-/-} mice (Fig. 1b). Moreover, the CCL11-induced activation of CDK5 was reversed by GW766994 (10 μ M), a CCR3-specific antagonist [34], in a dose-dependent manner (Fig. 1c, d). These data

suggest that CCR3 expressed on hippocampal neurons is functional. After treatment of the hippocampal neuronal cultures (14 DIV) with CCL11 (10 nM) for different time intervals, we observed that CCL11 treatment resulted in a time-dependent increase in the phosphorylation of CDK5 and GSK3 β ; the latter also plays an important role in AD pathogenesis [19]. Notably, the phosphorylations of CDK5 and GSK3 β were reversed by the pre-treatment of the neurons with GW766994 (10 μ M), a CCR3-specific antagonist [34], suggesting that these signaling pathways are mediated by CCR3 (Fig. 1e, f). Tau hyperphosphorylation, predominantly mediated by CDK5 and GSK3 β , is a major hallmark of AD. We observed that treatment of hippocampal neurons (14 DIV) with CCL11 (10 nM) for 15 min resulted in increased phosphorylation of tau at several sites tested, including T181, T205, S235, and S199, and these increases were reversed by a 1-h pre-treatment of the neurons with GW766994 (10 μ M) (Fig. 1g, h).

We also examined the effect of CCL11 on A β production in neurons. Starting at day 14 in vitro, primary hippocampal neuronal cells were treated with either vehicle or different concentrations of CCL11 for 48 h. Significant dose-dependent increase in A β _{1–42} secretion was observed in the CCL11-treated cells, and this effect was blocked by the pre-treatment with GW766994 (10 μ M) (Fig. 1i). A β _{1–40} levels also appeared to be increased in response to CCL11 treatment, but this effect did not reach statistical significance (Fig. 1j). To compensate for any uneven evaporation of the media, a Bradford protein assay was performed on media samples and data are presented as pmol A β /100 μ g protein (Fig. 1i, j).

Finally, we assessed the effect of CCL11 on neuronal morphology. Hippocampal neurons (14 DIV) expressing EGFP were treated with or without CCL11 (10 nM) in the presence or absence of GW766994 (10 μ M), and dendritic complexity and dendritic spine density were assessed. We observed that CCL11 treatment resulted in a significant decrease in the number of dendritic crossing (Fig. 1k, l) and a marked decrease in the density of dendritic spines (Fig. 1m, n). Intriguingly, these decreases were reversed by the pre-treatment of GW766994 (Fig. 1k–n).

Increased Expression of CCL11 and CCR3 in the Brain of APP/PS1 Double-Transgenic Mice The deleterious effects of CCL11 on the neuronal structure and functions described above leads to the hypothesis that CCL11/CCR3 plays a role in the pathology of AD via pathways beyond their detrimental effects on neurogenesis that has been reported previously [39]. To this end, we attempted to examine the expression of CCL11/CCR3 in the hippocampal CA1 region (Fig. 2a) of WT and APP/PS1 double-transgenic mice, a widely used AD mouse model. We observed that CCR3 was expressed in the hippocampal neurons of both WT and APP/PS1 double-transgenic mice, and its expression levels gradually elevated

with the age increase. Intriguingly, though the expression level of CCR3 was comparable at early ages (2–6 months old), a more robust age-dependent increase in its expression was observed in APP/PS1 double-transgenic mice relative to WT littermates (Fig. 2b, c). We also observed an increased level of CCL11, predominantly expressed by activated microglia (Fig. 2d), in the CSF of both APP/PS1 double-transgenic mice and WT littermates in an age-dependent manner, with a faster increase in APP/PS1 mice than in WT littermates (Fig. 2e).

CCR3 Deficiency Reduces A β Production and Deposition and the Associated Microgliosis and Astrogliosis in APP/PS1 Double-Transgenic Mice

To examine the effect of CCR3 on A β production and deposition in an AD mouse model, we crossed CCR3^{-/-} mice with APP/PS1 double-transgenic mice to generate APP/PS1/CCR3^{-/-} triple-mutant mice and their littermates, including WT, APP/PS1, and CCR3^{-/-}. We compared A β deposition and associated gliosis in the brains of these animals (12 months old). Immunohistochemistry with an antibody against A β 42 and the following stereological analysis indicated that A β deposits, which were undetectable in WT and CCR3^{-/-} mice (data not shown), were found in both the cortex and hippocampus of APP/PS1 double-transgenic and APP/PS1/CCR3^{-/-} triple-mutant mice, but the density of A β deposits was significantly lower in APP/PS1/CCR3^{-/-} triple-mutant mice compared to APP/PS1 littermates (Fig. 3a, b). To examine whether the decrease in A β deposition is attributable to the decreased production of A β in APP/PS1/CCR3^{-/-} triple-mutant mice, we measured the protein levels of A β monomer and oligomer forms in the hippocampal lysates of APP/PS1/CCR3^{-/-} triple-mutant mice (12 months old) and APP/PS1, CCR3^{-/-}, and WT littermates. We observed that in the hippocampus of APP/PS1/CCR3^{-/-} triple-mutant mice and APP/PS1 littermates, the vast majority of A β forms were ~40 mer, ~20 mer, tetramer, and trimer, with modest level of monomer. Intriguingly, significant reductions of A β trimer, tetramer, and ~40 mer were observed in APP/PS1/CCR3^{-/-} triple-mutant mice compared to APP/PS1 littermates (Fig. 3c). In this AD mouse model, A β deposits are surrounded by activated astrocytes and microglia (Fig. 3d, f), namely astrogliosis and microgliosis, which are believed to be the main sources of neuroinflammation. Intriguingly, markedly reduced astrogliosis (Fig. 3d, e) and microgliosis (Fig. 3f, g) were observed in APP/PS1/CCR3^{-/-} triple-mutant mice compared to that in APP/PS1 littermates.

CCR3 Deficiency Reduces Tau Hyperphosphorylation and the Activation of Tau Kinases in APP/PS1 Double-Transgenic Mice

Hyperphosphorylation of tau, a substrate for several protein kinases [21, 37], is phosphorylated at over 38 serine/threonine residues in AD [15, 32] and appears in AD mouse models after the onset of A β deposition [9, 23].

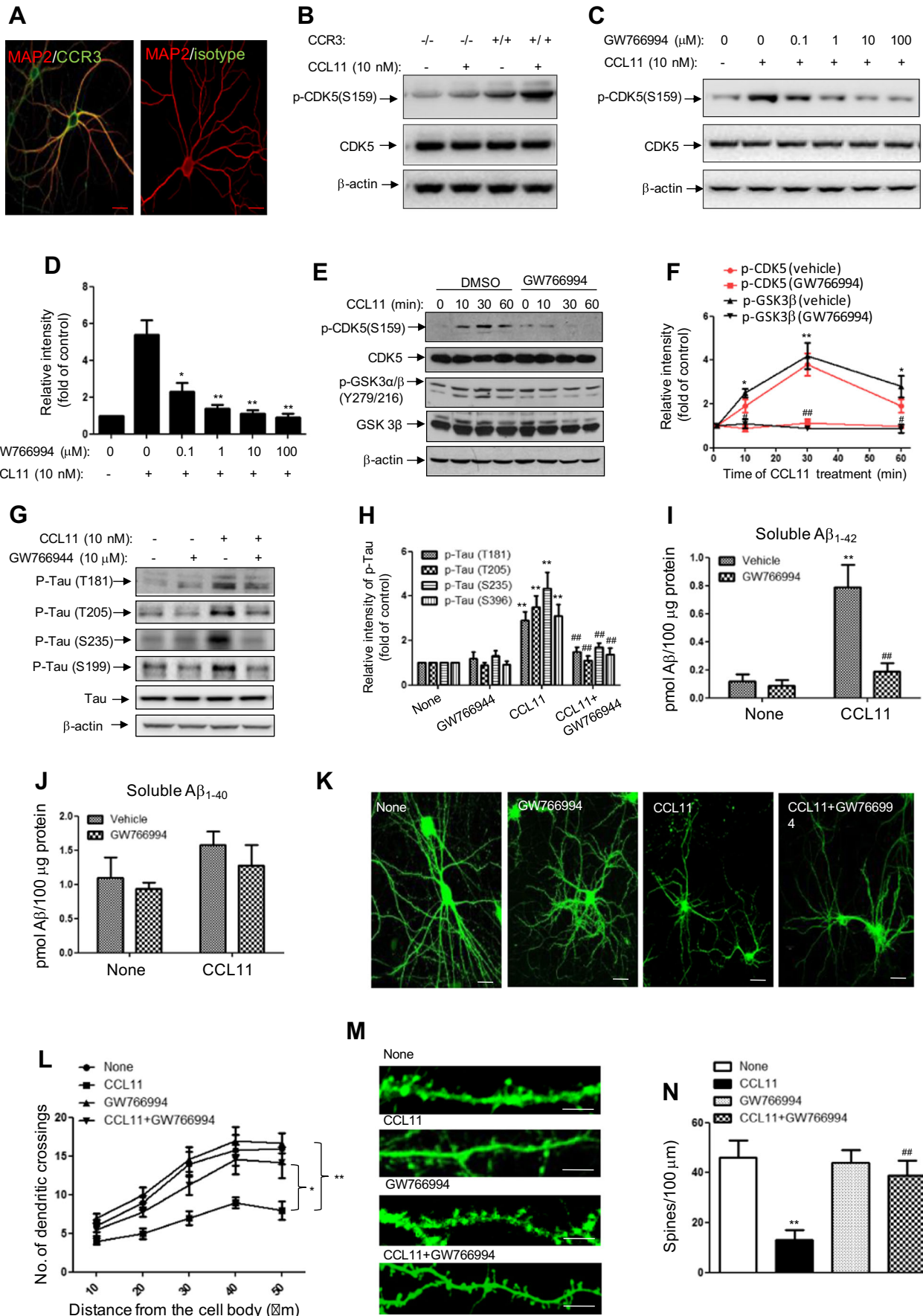


Fig. 1 CCL11 induces CDK5 and GSK3 β activation, tau phosphorylation, A β production, and dendritic spine loss in hippocampal neurons through activating CCR3. **a** Immunofluorescent image showing co-localization of CCR3 with MAP2 in hippocampal neuronal cultures (14 days in vitro). Shown are representative results from three independent experiments. Scale bar = 50 μ m. **b** Western blots of phosphorylated CDK5 (Ser159) and CDK5 in the cell lysate of hippocampal neuronal cultures (14 DIV) derived from WT or CCR3^{-/-} mice in the absence or presence of CCL11 (10 nM) for 30 min. Shown are representative results from three independent experiments. **c** Western blots of phosphorylated CDK5 (Ser159) and CDK5 in the cell lysate of hippocampal neuronal cultures (14 DIV) treated with or without CCL11 (10 nM) for 30 min in the absence or presence of different concentrations of GW766994 indicated. Shown are representative results from three independent experiments. **d** Quantitative analysis of phosphorylated-CDK5 (p-CDK5). Quantified results, normalized to CDK5 were expressed as folds of the values from the cells without treatment. Data (mean \pm SEM) were from three independent experiments. Differences were analyzed by one-way ANOVA. * p \leq 0.05; ** p \leq 0.01, compared with group without treatment. **e** Western blots of phosphorylated CDK5 (Ser159), CDK5, phosphorylated GSK3 α/β (Tyr216), and GSK3 β in the cell lysate of hippocampal neuronal cultures (14 days in vitro) treated with or without CCL11 (10 nM) for different time intervals in the absence or presence of GW766994 (10 μ M). Shown are representative results from three independent experiments. **f** Quantitative analysis of phosphorylated-CDK5 (p-CDK5) and phosphorylated GSK3 β (p-GSK3 β). Quantified results, normalized to CDK5 and GSK3 β , respectively, were expressed as folds of the values from the cells without treatment (time zero). Data (mean \pm SEM) were from three independent experiments. Differences were analyzed by one-way ANOVA. * p < 0.05; ** p < 0.01, compared with time zero in the same treatment group. # p < 0.05; ### p < 0.01, compared with the cells treated with vehicle. **g** Western blots of phosphorylated tau at T181, T205, Ser235, Ser396 in the cell lysate of hippocampal neuronal cultures treated with CCL11 (10 nM) for 10 min in the absence or presence of GW766994 (10 μ M). Shown are representative results from three independent experiments. **h** Quantitative analysis of phosphorylated tau at different phosphorylation sites indicated. Quantified results, normalized to total tau expression, were expressed as folds of the values from the cells without treatment (time zero). Data (mean \pm SEM) were from three independent experiments. Differences were analyzed by one-way ANOVA. * p < 0.05; ** p < 0.01, compared with time zero in the same treatment group. # p < 0.05; ### p < 0.01, compared with the cells treated with vehicle. **i** Effect of CCL11 on soluble A β 1–42 in primary hippocampal neuronal cultures. A β was measured by ELISA in media samples of vehicle- or CCL11-treated cells in the absence or presence of GW766994. Data (mean \pm SEM) were from three independent experiments. Differences were analyzed by one-way ANOVA. ** p < 0.01, compared with cells without any treatment (none). ### p < 0.01, compared with the cells treated with vehicle and CCL11. **j** Effect of CCL11 on soluble A β 1–40 in primary hippocampal neuronal cultures. A β was measured by ELISA in media samples of vehicle- or CCL11-treated cells in the absence or presence of GW766994. Data (mean \pm SEM) were from three independent experiments. No significant effect was observed for A β 1–40 although there was a trend for an increase in response to CCL11 treatment (p = 0.077). **k** Images of GFP-labeled mature hippocampal neurons (14 DIV). Shown are representative results from three independent experiments. **l** Sholl analysis of total number of branch point on basal dendrites of neurons treated with or without CCL11 (10 nM) in the absence or presence of GW766994 (10 μ M). Scale bar = 50 μ m. **m** Images of EGFP-labeled dendritic segments studded with mature spines from hippocampal neuronal cultures (14 DIV) treated with or without CCL11 (10 nM) in the absence or presence of GW766994 (10 μ M). Scale bars = 5 μ m. Shown are representative results from three independent experiments. **n** Quantitative assessment of spine densities determined in neurons without apparent dystrophies at 14 DIV neurons with the different treatments indicated. n = 10 culture/experiment and 600 spines from each condition. Data represent mean \pm SEM. Differences were analyzed by one-way ANOVA followed by Newman-Kuls test. ** p < 0.01, compared to the cells without treatment, ### p < 0.01, compared with the cells treated with vehicle and CCL11

Consistent with the previous findings [8, 9], a marked increase in tau hyperphosphorylation at multiple sites, including T181, T205, S199, and S235, associated with significant activation of the tau kinases, including ERK1/2, CDK5, and GSK3 β , was observed in the hippocampal tissues of APP/PS1 double-transgenic mice compared with that in wild-type littermates (Fig. 4a–h). Intriguingly, APP/PS1/CCR3^{-/-} triple-mutant mice exhibited a significantly reduced hyperphosphorylation of tau and a markedly decreased activity of the tau kinases compared to the APP/PS1 double-transgenic mice (Fig. 4a–h). Using immunohistochemistry and stereological analyses with an antibody against p-tau (T181), we confirmed a marked decrease in p-tau-positive neurons in the hippocampus of APP/PS1/CCR3^{-/-} triple-mutant mice compared to that in APP/PS1 littermates (Fig. 4i, j).

CCR3 Deficiency Rescues Loss of Dendritic Spines and Synapses Observed in APP/PS1 Double-Transgenic Mice

One of the major hallmarks of AD is the loss of synapses in the cortical and hippocampal regions. The deleterious effect of CCL11 on dendritic spine stability in primary neuronal cultures leads to the hypothesis that CCL11/CCR3 plays a role in synaptic loss in AD mouse model. To this end, we first performed Golgi-Cox staining in the hippocampal slices to visualize and quantify dendritic spines in APP/PS1/CCR3^{-/-} triple-mutant mice (12 months old), APP/PS1, CCR3^{-/-}, and WT littermates. APP/PS1 mice exhibited a marked decrease in the density of dendritic spines relative to WT littermates. In contrast, a significant reversal of the dendritic spine loss was observed in APP/PS1/CCR3^{-/-} triple-mutant mice (Fig. 5a, b). Western blot analysis indicated dramatic decreases in the expression of drebrin and PSD95, the post-synaptic markers, in APP/PS1 mice compared to that in WT littermates, and these decreases were reversed by CCR3 deficiency (Fig. 5c–e). To further confirm the effect of CCR3 deficiency on synaptic density in the hippocampus, we performed an electron microscopy to visualize and quantify synapses. A significant decrease in the density of synapses was observed in APP/PS1 mice, compared to WT littermates. In contrast, a significant rescue of synaptic loss was observed in APP/PS1/CCR3^{-/-} triple-mutant mice (Fig. 5f, g).

CCR3 Deficiency Rescued Spatial Memory Deficits in APP/PS1 Double-Transgenic Mice

APP/PS1 double-transgenic mice develop AD-like cognitive deficits in the advanced age [9]. The rescuing effect of CCR3 deficiency on synaptic loss observed in APP/PS1 mice leads to the hypothesis that CCR3 deficiency may rescue learning and memory deficits in the AD mouse model. To this end, we performed Morris water maze test, the most widely accepted behavioral test of hippocampus-dependent spatial learning and memory [33], to compare learning and memory tasks in APP/PS1/CCR3^{-/-} triple-mutant mice (12 months old) and their

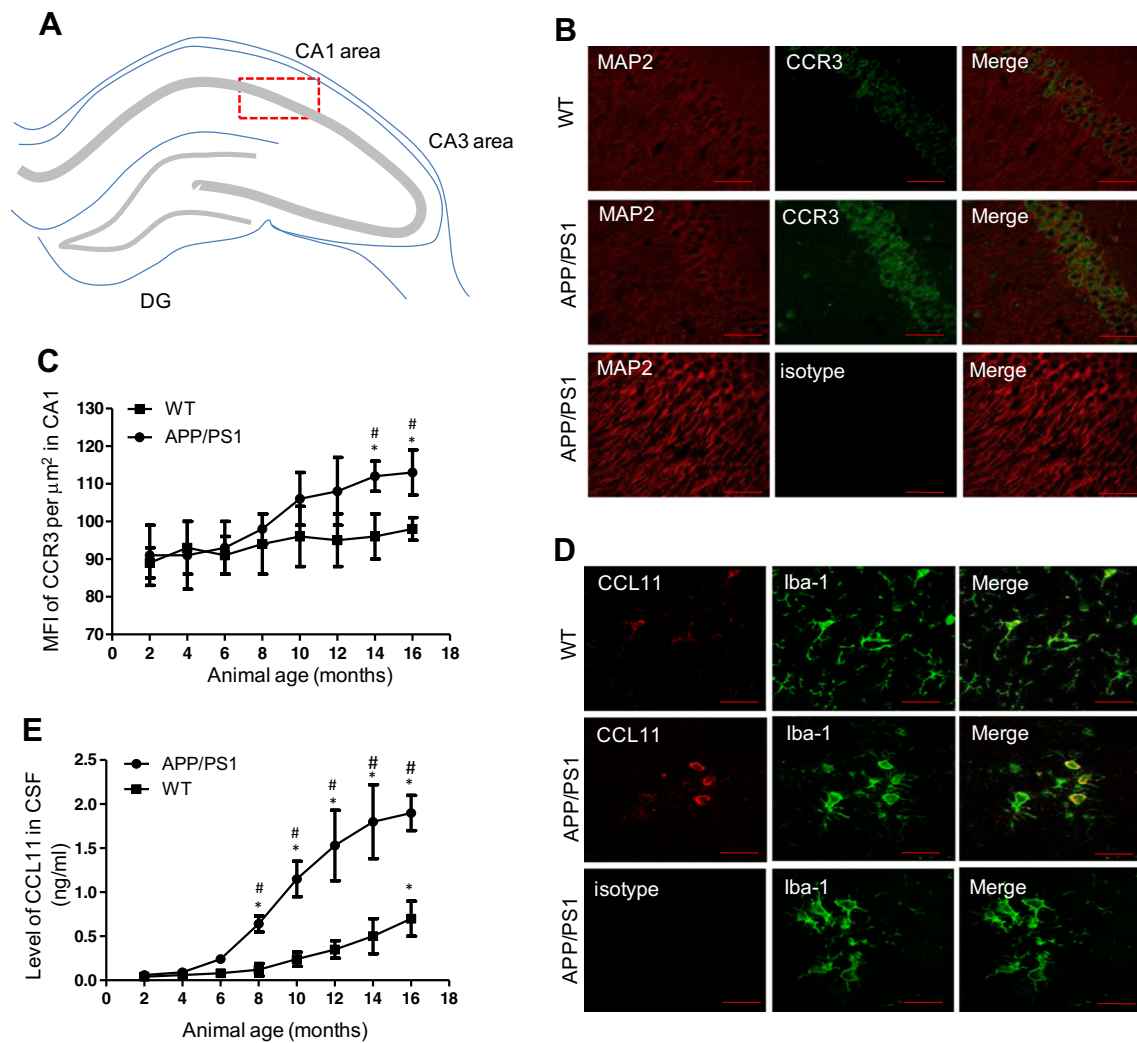


Fig. 2 Expression of CCL11/CCR3 in the brain tissues. **a** A diagram showing the CA1 region in which the expression of CCR3 was examined using immunohistochemistry and confocal microscopy. **b** Representative confocal images showing the co-immunostaining of CCR3 (green) and MAP2 (red) with a mixture of anti-MAP2 and anti-CCR3 or isotype IgG in the hippocampal CA1 region in the brains of WT and APP/PS1 transgenic mice (12 months old). Scale bar = 50 μm . **c** Quantitative assessment of the mean fluorescence intensity (MFI) of CCR3 in the hippocampal CA1 region of WT ($n = 10$) and APP/PS1 double-transgenic mice ($n = 10$). Data were mean \pm SEM. Differences were analyzed by one-way ANOVA followed by Newman-Kuls test.

* $p < 0.05$, compared with initial time point (2 months). # $p < 0.05$, compared with WT mice. **d** Representative confocal images showing the co-immunostaining of CCL11 (red) and Iba-1 (green) with a mixture of anti-Iba-1 and anti-CCL11 or isotype IgG in the brains of WT and APP/PS1 transgenic mice (12 months old). Scale bar = 50 μm . **e** ELISA analysis of CCL11 in the CSF of WT ($n = 10$) and APP/PS1 double-transgenic mice ($n = 10$). Data were mean \pm SEM. Differences were analyzed by one-way ANOVA. * $p < 0.05$, compared with initial time point (2 months). # $p < 0.05$, compared with WT control mice

littermates. The APP/PS1 mice exhibited impaired learning ability to use the available visuospatial cues to locate the submerged escape platform. In contrast, the APP/PS1/CCR3^{-/-} triple-mutant mice exhibited markedly improved learning capability in this task (Fig. 6a). Furthermore, we confirmed that CCR3 deficiency also significantly improved memory retention during the probe trial (Fig. 6b). It should be noted that the observed deficits in the capability of finding the submerged platform were not attributable to non-cognitive factors, because the four genotypes of mice displayed comparable

swimming speeds and escape latencies on the visible platform trails. These findings support the hypothesis that CCR3 deficiency may benefit from spatial memory deficits in APP/PS1 mice selectively, through preventing synaptic loss.

Discussion

Chemokines, elevated in the serum during aging and produced by activated glial cells in the process of neuroinflammation in

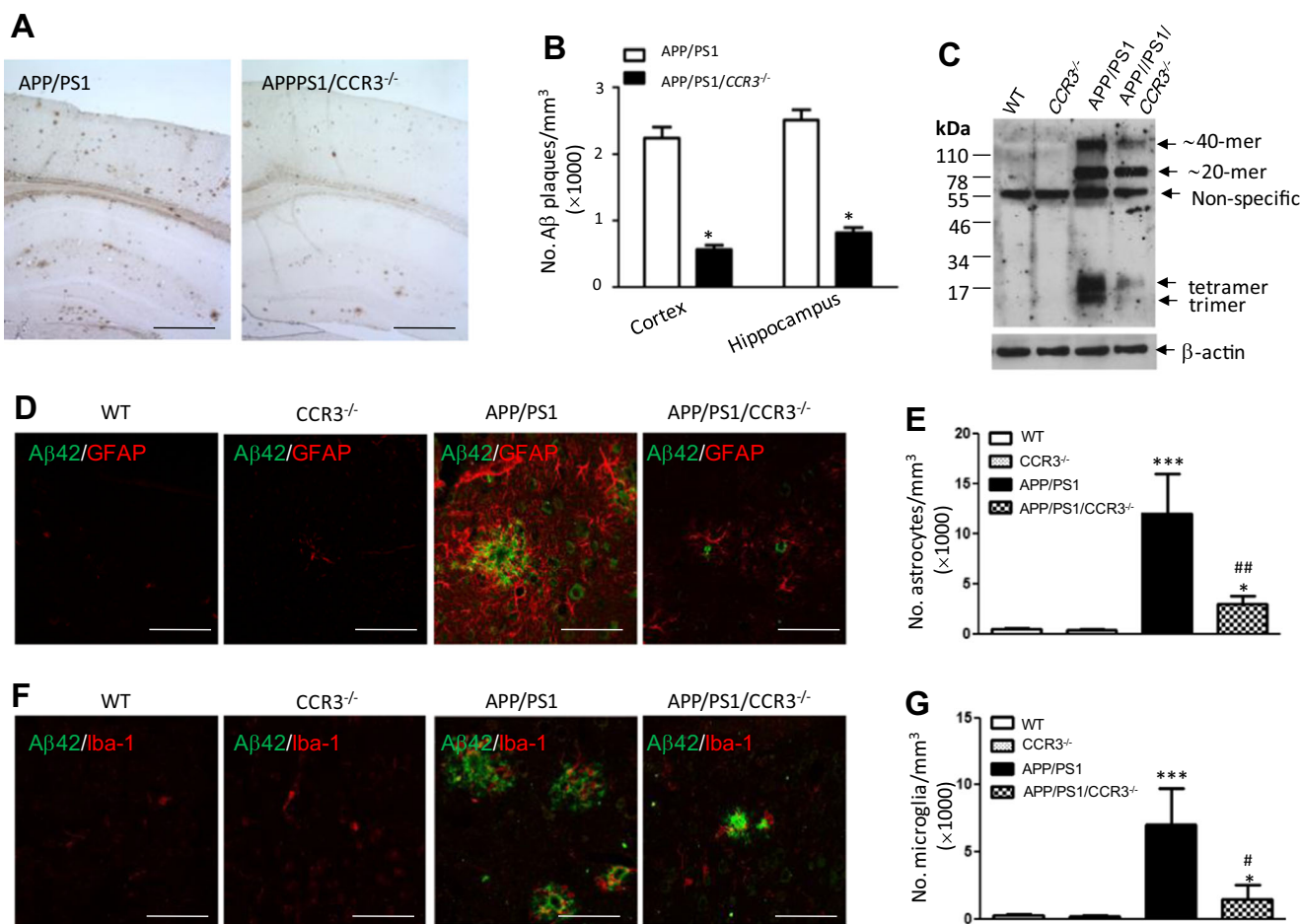


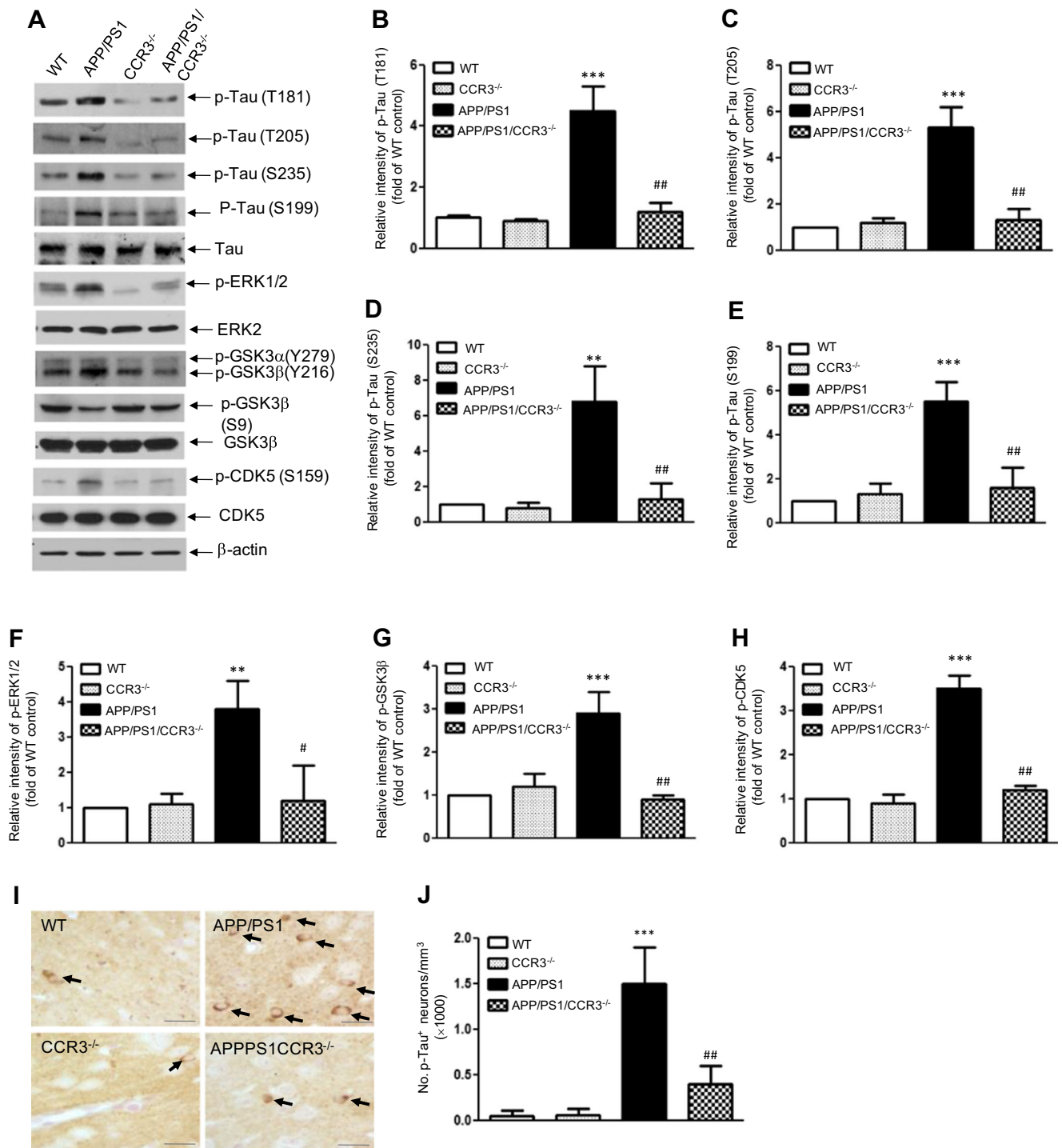
Fig. 3 CCR3 deficiency reduced A β production and deposition and the associated microgliosis and astrogliosis in APP/PS1 double-transgenic mice. **a** Representative immunohistochemistry images showing the reduced A β deposition in the cortical and hippocampal regions of APP/PS1/CCR3^{-/-} mice ($n = 10$) compared to APP/PS1 mice ($n = 10$). Scale bar = 100 μ m **b** Stereological analysis of A β deposits in the cortical and hippocampal regions of APP/PS1 double-transgenic mice ($n = 10$) and APP/PS1/CCR3^{-/-} triple-transgenic mice ($n = 10$). Data were mean \pm SEM. Differences were analyzed by one-way ANOVA followed by Newman-Kuels test. * $p < 0.05$; ** $p < 0.01$, compared with APP/PS1 double-transgenic mice. **c** Representative Western blots of APP and CTF in the lysates of WT ($n = 10$), CCR3^{-/-} ($n = 10$), APP/PS1 double-transgenic mice ($n = 10$), and APP/PS1/CCR3^{-/-} triple-transgenic mice ($n = 10$). **d** Representative co-immunofluorescent staining of A β and GFAP in the hippocampi of WT ($n = 10$), CCR3^{-/-} ($n = 10$), APP/PS1 double-transgenic mice ($n = 10$), and APP/PS1/CCR3^{-/-} triple-transgenic mice ($n = 10$). Scale bar = 50 μ m. **e**

Stereological analysis of GFAP-positive cells in the cortical and hippocampal regions of WT ($n = 10$), CCR3^{-/-} ($n = 10$), APP/PS1 double-transgenic mice ($n = 10$), and APP/PS1/CCR3^{-/-} triple-transgenic mice ($n = 10$). Data were mean \pm SEM. Differences were analyzed by one-way ANOVA followed by Newman-Kuels test. * $p < 0.05$, *** $p < 0.001$ compared with WT mice; ## $p < 0.01$, compared with APP/PS1 double-transgenic mice. **f** Representative co-immunofluorescent staining of A β and Iba-1 in the hippocampi of WT ($n = 10$), CCR3^{-/-} ($n = 10$), APP/PS1 double-transgenic mice ($n = 10$), and APP/PS1/CCR3^{-/-} triple-transgenic mice ($n = 10$). **g** Stereological analysis of Iba-1-positive cells in the cortical and hippocampal regions of WT ($n = 10$), CCR3^{-/-} ($n = 10$), APP/PS1 double-transgenic mice ($n = 10$), and APP/PS1/CCR3^{-/-} triple-transgenic mice ($n = 10$). Data were mean \pm SEM. Differences were analyzed by one-way ANOVA followed by Newman-Kuels test. * $p < 0.05$, *** $p < 0.001$ compared with WT mice; # $p < 0.05$, compared with APP/PS1 double-transgenic mice

AD brain, are attracting increasing attention with regard to their role in neurodegeneration. In the present study, we demonstrate that CCL11 induced marked activation of CDK5 and GSK-3 β in hippocampal neuronal cultures, associated with elevated phosphorylation of tau, enhanced production of A β , and accelerated dendritic spine loss. An age-dependent increase in the expression of CCL11 in microglia was evident in APP/PS1 transgenic mice. We further demonstrated that deficiency of CCR3, the receptor for CCL11, significantly

reduced A β production and the associated microgliosis and astrogliosis, tau hyperphosphorylation, and synaptic loss, associated with improvement of learning and memory performance, in APP/PS1 double-transgenic mice. Thus, the age-related increase in CCL11 may be directly involved in AD pathogenesis.

In the brains of AD patients, tau is abnormally hyperphosphorylated, and in this altered state, it is aggregated into paired helical filaments which form neurofibrillary



tangles. It is postulated that tau hyperphosphorylation at different sites has a different impact on its biological function and on its pathogenic roles. While hyperphosphorylation of tau at Ser262, Thr231, and Ser235 inhibits its binding to microtubules [36], hyperphosphorylation of tau at Ser199/Ser202/Thr205, Thr212, Thr231/Ser235, Ser262/Ser356, and Ser422 converts tau to an inhibitory molecule that sequesters normal microtubule-associated proteins from microtubules

[1]. Moreover, the density of neurofibrillary tangles in the neocortex correlates with dementia [43]. Thus, development of rational tau-based therapeutic drugs requires identifying the triggers of abnormal hyperphosphorylation of tau and understanding the underlying mechanisms. Chemokines appear to be important factors involved in tau pathologies. For instance, CXCL1 triggers tau hyperphosphorylation in primary neuronal cultures through

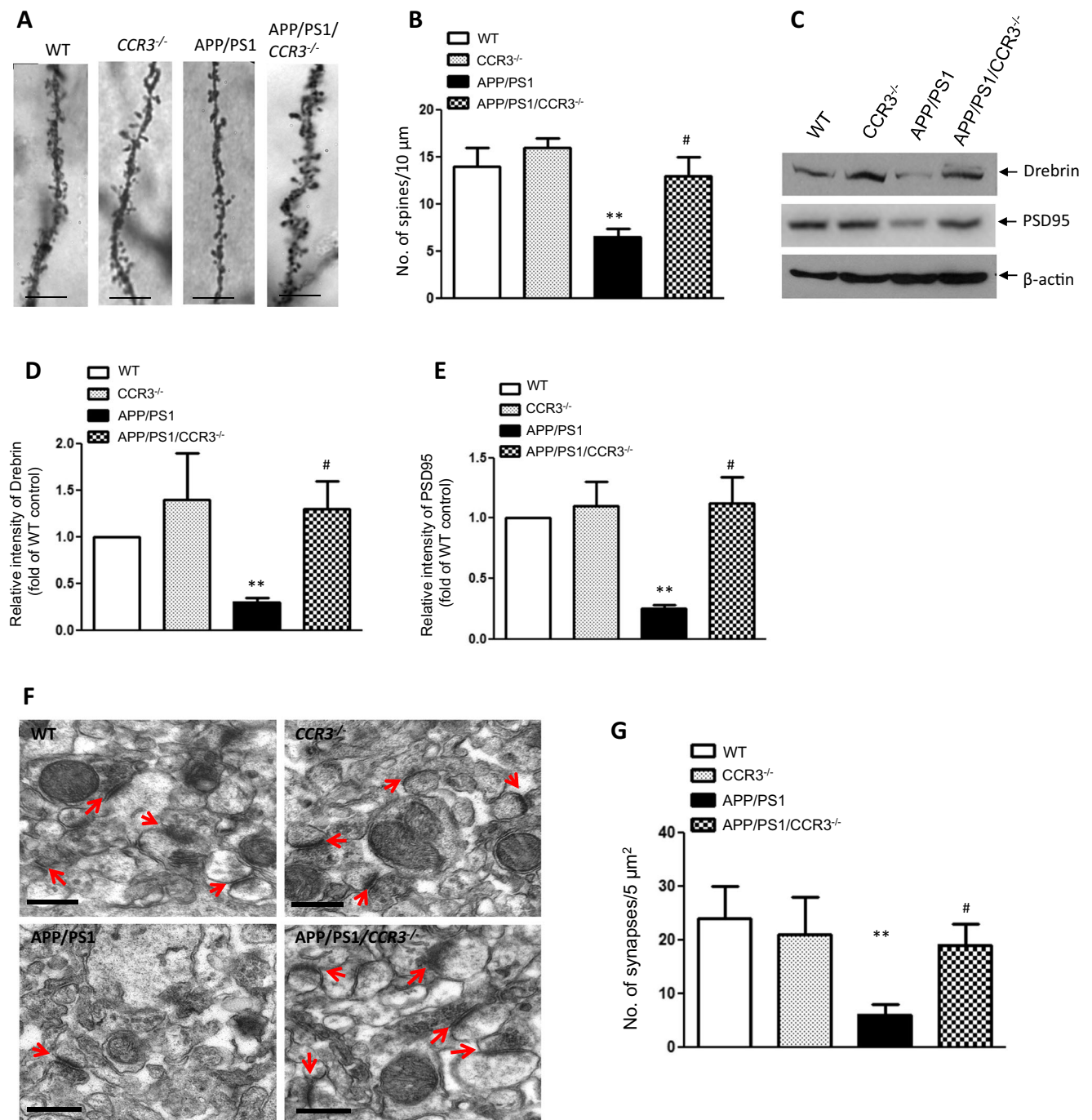
Fig. 4 CCR3 deficiency reduced tau hyperphosphorylation and the activation of the associated kinases in APP/PS1 double-transgenic mice. **a** Representative Western blots of phosphorylated Tau at T181, T205, S235, S199 total Tau, phosphorylated CDK5 (Ser159), CDK5, phosphorylated ERK1/2, ERK2, phosphorylated GSK3 α/β (Tyr276/216), and GSK3 β in the hippocampal lysates of WT ($n = 10$), CCR3 $^{-/-}$ ($n = 10$), APP/PS1 double-transgenic mice ($n = 10$), and APP/PS1/CCR3 $^{-/-}$ triple-transgenic mice ($n = 10$). Significant elevations of the phosphorylations of CDK5, GSK3 β , ERK1/2, and Tau at multiple phosphorylation sites indicated were observed in APP/PS1 double-transgenic mice, and these elevations were reversed in APP/PS1/CCR3 $^{-/-}$ triple-transgenic mice. **b–h** Quantitative assessments of the Western blots of phosphorylated Tau at T181, T205, S235, and S199, and the phosphorylated ERK1/2, GSK3 β , and CDK5, respectively, in the lysates of WT ($n = 10$), CCR3 $^{-/-}$ ($n = 10$), APP/PS1 double-transgenic mice ($n = 10$), and APP/PS1/CCR3 $^{-/-}$ triple-transgenic mice ($n = 10$). Data were mean \pm SEM. Differences were analyzed by one-way ANOVA. $**P \leq 0.01$, $***p < 0.001$ compared with WT mice; $\#p < 0.05$, $\#\#p < 0.01$, compared with APP/PS1 double-transgenic mice. **i** Representative immunohistochemistry image of phosphorylated Tau at T181 in the hippocampal CA1 regions of WT ($n = 10$), CCR3 $^{-/-}$ ($n = 10$), APP/PS1 double-transgenic mice ($n = 10$), and APP/PS1/CCR3 $^{-/-}$ triple-transgenic mice ($n = 10$). Scale bar = 50 μ m. **j** Stereological analysis of p-Tau-positive neurons in the hippocampal regions of WT ($n = 10$), CCR3 $^{-/-}$ ($n = 10$), APP/PS1 double-transgenic mice ($n = 10$), and APP/PS1/CCR3 $^{-/-}$ triple-transgenic mice ($n = 10$). Data were mean \pm SEM. Differences were analyzed by one-way ANOVA followed by Newman-Kuls test. $***p < 0.001$ compared with WT mice; $\#\#p < 0.01$, compared with APP/PS1 double-transgenic mice

CXCR2 (CXCL1 receptor)-mediated ERK1/2 activation [45], and a recent study further showed that treatment of long-term neuronal cultures with CXCL1 resulted in tau cleavage in a caspase-3-dependent manner [47]. Now, we provide evidence for the first time that CCL11/CCR3 plays a causative role in tau hyperphosphorylation. Based on the observation that nanomolar concentration of CCL11 directly induced tau phosphorylation in primary neuronal cultures, we propose that the age-dependent increase in CCL11 is a potential risk factor for AD. In support of this notion, we observed that CCR3 deficiency reversed tau hyperphosphorylation in APP/PS1 double-transgenic mice. It should be noted that given the previous findings that CCR3 is expressed by microglia and plays a role in microglial activation [17], which is known to promote tau hyperphosphorylation via secreting pro-inflammatory cytokines [28], we cannot exclude the possibility that the CCL11/CCR3 may also cause tau hyperphosphorylation via activating microglia in AD brain. Several protein kinases, especially CDK5 and GSK3 β , are believed to regulate tau phosphorylation in the brain [27]. Intriguingly, our results demonstrate that CCL11 induced activation of both CDK5 and GSK3 β in neuronal cultures, and CCR3 deficiency reversed the increased phosphorylation of both CDK5 and GSK3 β in the brains of APP/PS1 double-transgenic mice. Our studies establish the pathways through which CCL11/CCR3 triggers tau hyperphosphorylation.

In addition to tau pathology, senior plaques composed of A β deposits and the surrounding activated microglia and astrocytes is another important hallmark of AD. A β peptides, produced via the cleavage of APP by the β - and γ -secretases, aggregate and form A β deposits in the brain. γ -secretase cleaves the APP C-terminal fragment into two major forms of A β polypeptides, A β 40 and A β 42. The relative amount of A β 42 is particularly critical for AD progression because it is more prone to aggregation than A β 40 peptide [5, 20, 42]. However, triggers of APP processing and A β production remain largely unclear in sporadic AD population. In the present study, we demonstrate that CCL11 induced a marked increase in the production of A β 42, with modest effect on the production of A β 40, in primary neuronal cultures, in a CCR3-dependent manner. In support of the in vitro findings, we observed that CCR3 deficiency significantly reduced the levels of A β , predominantly its oligomeric forms, in the brains of APP/PS1 double-transgenic mice. Given the previous findings for the age-dependent elevation of serum CCL11 [40], which is known to penetrate the blood-brain barrier [12], it reasonably hypothesizes that the increasing CCL11 is a risk factor of A β production in the brain and early interfering CCL11/CCR3 may delay the onset of AD. However, mechanisms by which CCL11 promotes A β production remain unclear. Previous studies have revealed that the chemokine CXCL1 enhances γ -secretase activity and promotes A β production via CXCR2 receptor [2], and the deletion of CXCR2 inhibits γ -secretase activity and A β production in a murine model of AD [3]. Whether similar mechanisms are employed by CCL1/CCR3 to promote A β production will be investigated in our future studies.

A β deposits are believed to be a major trigger of microgliosis and astrogliosis, both of which contribute to neuroinflammation that has long been postulated to play a critical role in the pathogenesis of AD [31]. We observed that CCR3 deficiency significantly reduced microgliosis and astrogliosis, suggesting that early intervention of CCL11/CCR3 could attenuate neuroinflammation in the brains of AD patients. The reduced neuroinflammation in the APP/PS1/CCR3 $^{-/-}$ triple-mutant mice could be attributed to at least two pathways. First, deletion of CCR3 reduces A β deposits, which are known to activate microglia and astrocytes, thereby attenuating microgliosis and astrogliosis. Second, CCR3 is expressed by microglia and plays a role in microglial activation [17], thus its deficiency may prevent microglial activation.

The most intriguing finding in the present study is that CCR3 deficiency rescued synaptic loss and spatial memory deficits in APP/PS1 mice. Though the attenuated synaptic loss and improved spatial learning observed in the CCR3-deficient APP/PS1 double-transgenic mice could be



attributed to the reduced A β and neuroinflammation, both of which contribute to synaptic loss and cognitive deficits in AD [35, 41], based on the findings that CCL11 reduced dendritic spines in primary neuronal cultures, we propose a direct role of CCL11/CCR3 in the synaptic loss observed in the AD mouse model. Before the present study, several other chemokines have been reported to interfere with synaptic transmission or plasticity. For instance, CCL3 reduces basal synaptic transmission at the Schaffer collateral-CA1 synapse and significantly impairs long-term potentiation, an effect

abolished by Maraviroc, a CCR5-specific antagonist [29]. CCL2 modulates neuronal excitability and synaptic transmission in rat hippocampal slices [48]. However, mechanisms through which chemokines modulate synaptic structure and functions remain largely unknown. Nevertheless, these findings increase the importance for investigating the role of chemokines in the cognitive deficits in AD.

In summary, the presented data demonstrate for the first time that CCL11/CCR3 plays a role in A β production, tau hyperphosphorylation, and synaptic loss, all of

Fig. 5 CCR3 deficiency rescued loss of dendritic spines and synapses observed in APP/PS1 double-transgenic mice. **a** Representative Golgi-Cox staining showing the dendritic spines in the hippocampal CA1 region of WT ($n = 10$), $CCR3^{-/-}$ ($n = 10$), APP/PS1 double-transgenic mice ($n = 10$), and APP/PS1/ $CCR3^{-/-}$ triple-transgenic mice ($n = 10$). Scale bar = 5 μm . **b** Quantitative assessment of dendritic spines in the hippocampal CA1 region of WT ($n = 10$), $CCR3^{-/-}$ ($n = 10$), APP/PS1 double-transgenic mice ($n = 10$), and APP/PS1/ $CCR3^{-/-}$ triple-transgenic mice ($n = 10$). Data were mean \pm SEM. $**p < 0.01$ compared with WT mice; $\#p < 0.05$, compared with APP/PS1 double-transgenic mice. **c** Representative Western blots of Drebrin and PSD95 in the lysates of WT ($n = 10$), $CCR3^{-/-}$ ($n = 10$), APP/PS1 double-transgenic mice ($n = 10$) and APP/PS1/ $CCR3^{-/-}$ triple-transgenic mice ($n = 10$). The experiments were performed for three times, with similar results. **d, e** Quantitative assessments of the Western blots of Drebrin and PSD95 in the lysates of WT ($n = 10$), $CCR3^{-/-}$ ($n = 10$), APP/PS1 double-transgenic mice ($n = 10$), and APP/PS1/ $CCR3^{-/-}$ triple-transgenic mice ($n = 10$), respectively. Data were mean \pm SEM. Differences were analyzed by one-way ANOVA. $**p < 0.01$ compared with WT mice; $\#p < 0.05$, compared with APP/PS1 double transgenic mice. **f** Representative electron microscopy images showing synapses (arrows indicated) in the hippocampal CA1 region of WT ($n = 10$), $CCR3^{-/-}$ ($n = 10$), APP/PS1 double-transgenic mice ($n = 10$), and APP/PS1/ $CCR3^{-/-}$ triple-transgenic mice ($n = 10$). Scale bar = 10 nm. **g** Quantitative assessment of synapses in the hippocampal CA1 region of WT ($n = 10$), $CCR3^{-/-}$ ($n = 10$), APP/PS1 double-transgenic mice ($n = 10$), and APP/PS1/ $CCR3^{-/-}$ triple-transgenic mice ($n = 10$). Data were mean \pm SEM. Differences were analyzed by one-way ANOVA followed by Newman-Kuls test. $**p < 0.01$ compared with WT mice; $\#p < 0.05$, compared with APP/PS1 double-transgenic mice

which are important contributors of AD pathogenesis. Though the underlying mechanisms remain incompletely understood, CCL11-induced activation of protein kinases

especially CDK5 and GSK3 β may contribute generally to the above deleterious effects, as deregulation of Cdk5 and GSK3 β contributes to an array of pathological events in AD, ranging from formation of neurofibrillary tangles, senile plaques, synaptic damage, as well as neuronal cell apoptosis [7, 26]. Given the age-dependent increase in CCL11, it is reasonable to hypothesize that CCL11 is a risk factor in AD, and early prevention of its elevation may delay the age at onset of AD. It should be noted that though deletion of CCR3 in APP/PS1 double-transgenic mice significantly reduced the AD-related pathologies, suggesting an important role of CCL11/CCR3 in the pathogenesis of AD, we cannot exclude the possible involvement of other CCR3 binding chemokines, such CCL26, CCL7, CCL13, and CCL5, in the pathogenesis of AD. Nevertheless, these data suggest that CCR3 antagonists are potential therapeutic agents for AD. This notion is supported by our data that GW766994, the specific CCR3 antagonist, was shown to inhibit A β production, tau phosphorylation, and dendritic spine loss in vitro. However, given the poor penetrability of the blood-brain-barrier of this compound, it was not suitable for in vivo study. In the future, brain-penetrable CCR3 antagonists need to be developed and evaluated in the AD mouse models. These studies may lead the development of novel therapeutic approaches for AD.

AD, Alzheimer's disease; A β , amyloid β ; APP, amyloid precursor protein; CDK5, cyclin-dependent protein kinase 5; DIV, days in vitro; GSK3 β , glypican synthesis kinase 3 β ; PS1, presenilin 1.

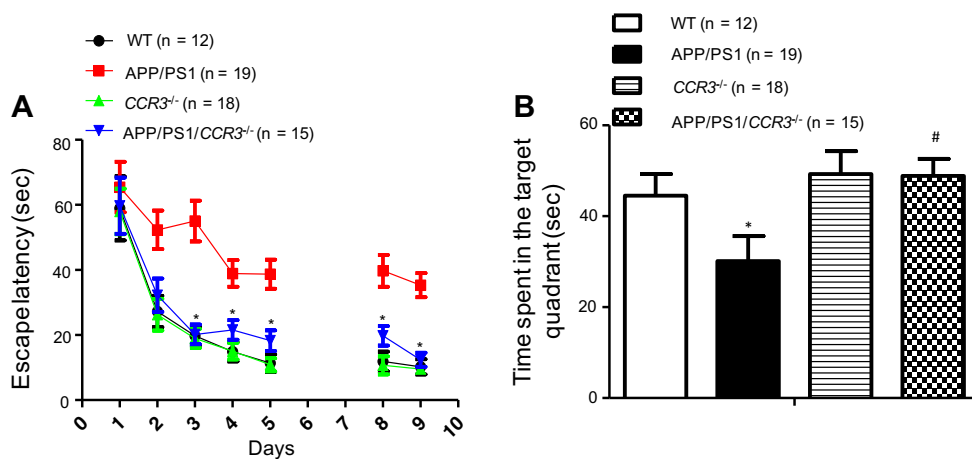


Fig. 6 CCR3 deficiency rescued spatial memory deficits in APP/PS1 double-transgenic mice. **a** Acquisition of spatial learning of WT ($n = 12$), $CCR3^{-/-}$ ($n = 18$), APP/PS1 double-transgenic mice ($n = 19$), and APP/PS1/ $CCR3^{-/-}$ triple-transgenic mice ($n = 15$) in the Morris water maze hidden-platform task. Learning deficits in APP/PS1 double-transgenic mice were reversed in APP/PS1/ $CCR3^{-/-}$ triple-mutant mice. Latency score represents time taken to escape to the platform from the

water. Data were mean \pm SEM. Differences were analyzed by one-way ANOVA. $*p < 0.05$, compared with APP/PS1 double-transgenic mice. **b** Memory test in Morris water maze probe trial without platform. Note that the deficits in APP/PS1 double-transgenic mice were reversed in APP/PS1/ $CCR3^{-/-}$ triple-mutant mice. Data were mean \pm SEM. Differences were analyzed by one-way ANOVA. $*p < 0.05$ compared with WT mice; $\#p < 0.05$, compared with APP/PS1 double transgenic mice

Acknowledgements We thank Dr. Guo-Huang Fan, professor in Tongji University for the helpful discussion. This work was supported by the National Natural Science Foundation of China (ID81371395), Liaoning Provincial Natural Science Foundation (ID 2015020547), and China Post-doctoral Science Foundation (ID 2015 M581375) to Yi Sui.

Author's Contribution YS designed the experiments, oversaw the whole project, and prepared the manuscript. CZ performed the experiments in Figs. 1, 2, and 5 and prepared the manuscript. BX performed the experiments in Figs. 3 and 4. XS performed the experiments in Fig. 6. QZ performed the experiments in Fig. 6

Compliance with Ethical Standards

Conflict of Interest The authors declare that they have no conflict of interest.

References

- Alonso Adel C, Mederlyova A, Novak M, Grundke-Iqbal I, Iqbal K (2004) Promotion of hyperphosphorylation by frontotemporal dementia tau mutations. *J Biol Chem* 279:34873–34881
- Bakshi P, Margenthaler E, Laporte V, Crawford F, Mullan M (2008) Novel role of CXCR2 in regulation of gamma-secretase activity. *ACS Chem Biol* 3:777–789
- Bakshi P, Margenthaler E, Reed J, Crawford F, Mullan M (2011) Depletion of CXCR2 inhibits gamma-secretase activity and amyloid-beta production in a murine model of Alzheimer's disease. *Cytokine* 53:163–169
- Brookmeyer R, Kawas CH, Abdallah N, Paganini-Hill A, Kim RC, and Corrada MM (2016) Impact of interventions to reduce Alzheimer disease pathology on the prevalence of dementia in the oldest-old. *Alzheimer's & dementia: the journal of the Alzheimer's Association*
- Burdick D, Soreghan B, Kwon M, Kosmoski J, Knauer M, Henschen A, Yates J, Cotman C et al (1992) Assembly and aggregation properties of synthetic Alzheimer's A4/beta amyloid peptide analogs. *J Biol Chem* 267:546–554
- Cho SH, Sun B, Zhou Y, Kauppinen TM, Halabisky B, Wes P, Ransohoff RM, Gan L (2011) CX3CR1 protein signaling modulates microglial activation and protects against plaque-independent cognitive deficits in a mouse model of Alzheimer disease. *J Biol Chem* 286:32713–32722
- Crews L, Masliah E (2010) Molecular mechanisms of neurodegeneration in Alzheimer's disease. *Hum Mol Genet* 19:R12–R20
- Ding Y, Qiao A, Fan GH (2010) Indirubin-3'-monoxime rescues spatial memory deficits and attenuates beta-amyloid-associated neuropathology in a mouse model of Alzheimer's disease. *Neurobiol Dis* 39:156–168
- Ding Y, Qiao A, Wang Z, Goodwin JS, Lee ES, Block ML, Allsbrook M, McDonald MP et al (2008) Retinoic acid attenuates beta-amyloid deposition and rescues memory deficits in an Alzheimer's disease transgenic mouse model. *J Neurosci Off J Soc Neurosci* 28:11622–11634
- Duan RS, Chen Z, Dou YC, Concha Quezada H, Nennesmo I, Adem A, Winblad B, Zhu J (2006) Apolipoprotein E deficiency increased microglial activation/CCR3 expression and hippocampal damage in kainic acid exposed mice. *Exp Neurol* 202:373–380
- Dumanis SB, Tesoriero JA, Babus LW, Nguyen MT, Trotter JH, Ladu MJ, Weeber EJ, Turner RS et al (2009) ApoE4 decreases spine density and dendritic complexity in cortical neurons in vivo. *J Neurosci Off J Soc Neurosci* 29:15317–15322
- Erickson MA, Morofuji Y, Owen JB, Banks WA (2014) Rapid transport of CCL11 across the blood-brain barrier: regional variation and importance of blood cells. *J Pharmacol Exp Ther* 349:497–507
- Facci L, Skaper SD (2012) Culture of rodent cortical and hippocampal neurons. *Methods Mol Biol* 846:49–56
- Fischer A, Sananbenesi F, Pang PT, Lu B, Tsai LH (2005) Opposing roles of transient and prolonged expression of p 25 in synaptic plasticity and hippocampus-dependent memory. *Neuron* 48:825–838
- Hanger DP, Betts JC, Loviny TL, Blackstock WP, Anderton BH (1998) New phosphorylation sites identified in hyperphosphorylated tau (paired helical filament-tau) from Alzheimer's disease brain using nano-electrospray mass spectrometry. *J Neurochem* 71:2465–2476
- Hasegawa-Ishii S, Inaba M, Li M, Shi M, Umegaki H, Ikehara S, and Shimada A (2015). Increased recruitment of bone marrow-derived cells into the brain associated with altered brain cytokine profile in senescence-accelerated mice. *Brain structure & function*
- He J, Chen Y, Farzan M, Choe H, Ohagen A, Gartner S, Busciglio J, Yang X et al (1997) CCR3 and CCR5 are co-receptors for HIV-1 infection of microglia. *Nature* 385:645–649
- Heppner FL, Ransohoff RM, Becher B (2015) Immune attack: the role of inflammation in Alzheimer disease. *Nat Rev Neurosci* 16:358–372
- Imahori K, Uchida T (1997) Physiology and pathology of tau protein kinases in relation to Alzheimer's disease. *J Biochem* 121:179–188
- Jarrett JT, Berger EP, Lansbury PT Jr (1993) The C-terminus of the beta protein is critical in amyloidogenesis. *Ann N Y Acad Sci* 695: 144–148
- Johnson GV, Hartigan JA (1999) Tau protein in normal and Alzheimer's disease brain: an update. *Journal of Alzheimer's disease: JAD* 1:329–351
- Katzman R, Saitoh T (1991) Advances in Alzheimer's disease. *FASEB journal: official publication of the Federation of American Societies for Experimental Biology* 5:278–286
- Kurt MA, Davies DC, Kidd M, Duff K, Howlett DR (2003) Hyperphosphorylated tau and paired helical filament-like structures in the brains of mice carrying mutant amyloid precursor protein and mutant presenilin-1 transgenes. *Neurobiol Dis* 14:89–97
- Lahiri DK, Chen D, Ge YW, Bondy SC, Sharman EH (2004) Dietary supplementation with melatonin reduces levels of amyloid beta-peptides in the murine cerebral cortex. *J Pineal Res* 36:224–231
- Le Thuc O, Blondeau N, Nahon JL, Rovere C (2015) The complex contribution of chemokines to neuroinflammation: switching from beneficial to detrimental effects. *Ann N Y Acad Sci* 1351:127–140
- Liu SL, Wang C, Jiang T, Tan L, Xing A and Yu JT (2015) The role of Cdk5 in Alzheimer's disease. *Molecular neurobiology*
- Lovestone S, Reynolds CH (1997) The phosphorylation of tau: a critical stage in neurodevelopment and neurodegenerative processes. *Neuroscience* 78:309–324
- Maphis N, Xu G, Kokiko-Cochran ON, Jiang S, Cardona A, Ransohoff RM, Lamb BT, Bhaskar K (2015) Reactive microglia drive tau pathology and contribute to the spreading of pathological tau in the brain. *Brain J Neurol* 138:1738–1755
- Marciniak E, Faivre E, Dutar P, Alves Pires C, Demeyer D, Caillierez R, Laloux C, Buee L et al (2015) The chemokine MIP-1alpha/CCL3 impairs mouse hippocampal synaptic transmission, plasticity and memory. *Scientific reports* 5:15862
- Mattson MP (2004) Pathways towards and away from Alzheimer's disease. *Nature* 430:631–639
- Morales I, Guzman-Martinez L, Cerda-Troncoso C, Farias GA, Maccioni RB (2014) Neuroinflammation in the pathogenesis of Alzheimer's disease. A rational framework for the search of novel therapeutic approaches. *Front Cell Neurosci* 8:112
- Morishima-Kawashima M, Hasegawa M, Takio K, Suzuki M, Yoshida H, Watanabe A, Titani K, Ihara Y (1995) Hyperphosphorylation of tau in PHF. *Neurobiol Aging* 16:365–371 discussion 371–380

33. Morris R (1984) Developments of a water-maze procedure for studying spatial learning in the rat. *J Neurosci Methods* 11:47–60
34. Neighbour H, Boulet LP, Lemiere C, Sehmi R, Leigh R, Sousa AR, Martin J, Dallow N et al (2014) Safety and efficacy of an oral CCR3 antagonist in patients with asthma and eosinophilic bronchitis: a randomized, placebo-controlled clinical trial. *Clinical and experimental allergy: journal of the British Society for Allergy and Clinical Immunology* 44:508–516
35. Rama Rao KV, Kielian T (2015) Neuron-astrocyte interactions in neurodegenerative diseases: role of neuroinflammation. *Clinical & experimental neuroimmunology* 6:245–263
36. Sengupta A, Kabat J, Novak M, Wu Q, Grundke-Iqbal I, Iqbal K (1998) Phosphorylation of tau at both Thr 231 and Ser 262 is required for maximal inhibition of its binding to microtubules. *Arch Biochem Biophys* 357:299–309
37. Singh TJ, Grundke-Iqbal I, McDonald B, Iqbal K (1994) Comparison of the phosphorylation of microtubule-associated protein tau by non-proline dependent protein kinases. *Mol Cell Biochem* 131:181–189
38. van der Meer P, Ulrich AM, Gonzalez-Scarano F, Lavi E (2000) Immunohistochemical analysis of CCR2, CCR3, CCR5, and CXCR4 in the human brain: potential mechanisms for HIV dementia. *Exp Mol Pathol* 69:192–201
39. Villeda SA, Luo J, Mosher KI, Zou B, Britschgi M, Bieri G, Stan TM, Fainberg N et al (2011) The ageing systemic milieu negatively regulates neurogenesis and cognitive function. *Nature* 477:90–94
40. Villeda SA, Plambeck KE, Middeldorp J, Castellano JM, Mosher KI, Luo J, Smith LK, Bieri G et al (2014) Young blood reverses age-related impairments in cognitive function and synaptic plasticity in mice. *Nat Med* 20:659–663
41. Viola KL, Klein WL (2015) Amyloid beta oligomers in Alzheimer's disease pathogenesis, treatment, and diagnosis. *Acta Neuropathol* 129:183–206
42. Walsh DM, Selkoe DJ (2007) A beta oligomers—a decade of discovery. *J Neurochem* 101:1172–1184
43. Wang JZ, Xia YY, Grundke-Iqbal I, Iqbal K (2013) Abnormal hyperphosphorylation of tau: sites, regulation, and molecular mechanism of neurofibrillary degeneration. *Journal of Alzheimer's disease: JAD* 33(Suppl 1):S123–S139
44. Wirenfeltd M, Dalmau I, Finsen B (2003) Estimation of absolute microglial cell numbers in mouse fascia dentata using unbiased and efficient stereological cell counting principles. *Glia* 44:129–139
45. Xia M, Hyman BT (2002) GROalpha/KC, a chemokine receptor CXCR2 ligand, can be a potent trigger for neuronal ERK1/2 and PI-3 kinase pathways and for tau hyperphosphorylation—a role in Alzheimer's disease? *J Neuroimmunol* 122:55–64
46. Xia MQ, Qin SX, Wu LJ, Mackay CR, Hyman BT (1998) Immunohistochemical study of the beta-chemokine receptors CCR3 and CCR5 and their ligands in normal and Alzheimer's disease brains. *Am J Pathol* 153:31–37
47. Zhang XF, Zhao YF, Zhu SW, Huang WJ, Luo Y, Chen QY, Ge LJ, Li RS et al (2015) CXCL1 triggers caspase-3 dependent tau cleavage in long-term neuronal cultures and in the hippocampus of aged mice: implications in Alzheimer's disease. *Journal of Alzheimer's disease: JAD* 48:89–104
48. Zhou Y, Tang H, Liu J, Dong J, Xiong H (2011) Chemokine CCL2 modulation of neuronal excitability and synaptic transmission in rat hippocampal slices. *J Neurochem* 116:406–414